Correction

PHARMACOLOGY

Correction for "CXCR4/YY1 inhibition impairs VEGF network and angiogenesis during malignancy," by Filomena de Nigris, Valeria Crudele, Alfonso Giovane, Amelia Casamassimi, Antonio Giordano, Hermes J. Garban, Francesco Cacciatore, Francesca Pentimalli, Diana C. Marquez-Garban, Antonella Petrillo, Letizia Cito, Linda Sommese, Andrea Fiore, Mario Petrillo, Alfredo Siani, Antonio Barbieri, Claudio Arra, Franco Rengo, Toshio Hayashi, Mohammed Al-Omran, Louis J. Ignarro, and Claudio Napoli, which was first published July 26, 2010; 10.1073/pnas.1008256107 (*Proc Natl Acad Sci USA* 107:14484–14489).

The authors wish to note the following: "Concerns about the presentation of data in some of the figures in our paper were brought to our attention. During the process of data checking by international ALCOA parameters, we detected mistakes during figure preparation of some in vitro results in Figs. 3*B* and 5 *A* and *C* and Fig. S3. We have been able to find many original autoradiographs to confirm the results reported in our paper. We apologize for the inconvenience for these honest errors, which, importantly, do not affect the main results of the study.

"In Fig. 3*B*, the first two bands of the VEGFB box look very similar, but at higher resolution, the bands are different. The original autoradiograph was found and the bands were presented in a horizontally inverted form during image assembly. In the VEGFC box, the first, second, and fourth bands look identical. During image assembly (cut and flipping the image) a copy of band 1 was inadvertently used instead of the correct image of band 4.

"In Fig. 5*A*, we admit similarity of the bands in the ERK 1/2 gel; however, we recovered another experiment performed at the same time as data reported in the paper showing that, in our experimental conditions, ERK protein expression did not change during the time-course experiment.

"In Fig. 5*C*, we admit to poor quality resolution of the published image and the appearance of two similar though irrelevant bands in the first two lanes. We apologize for the mistake due to erroneous duplication of bands during figure assembly. Data from other experiments performed at the time confirm the results and are used in the corrected figure.

"In Fig. S3, we inadvertently duplicated the panel of VEGFB for VEGFD and GADPH, but have found the correct original images, which confirmed our results."

The editors have reviewed the data from the authors and the corrected Fig. 3, Fig. 5, and Fig. S3, and their legends, appear below.

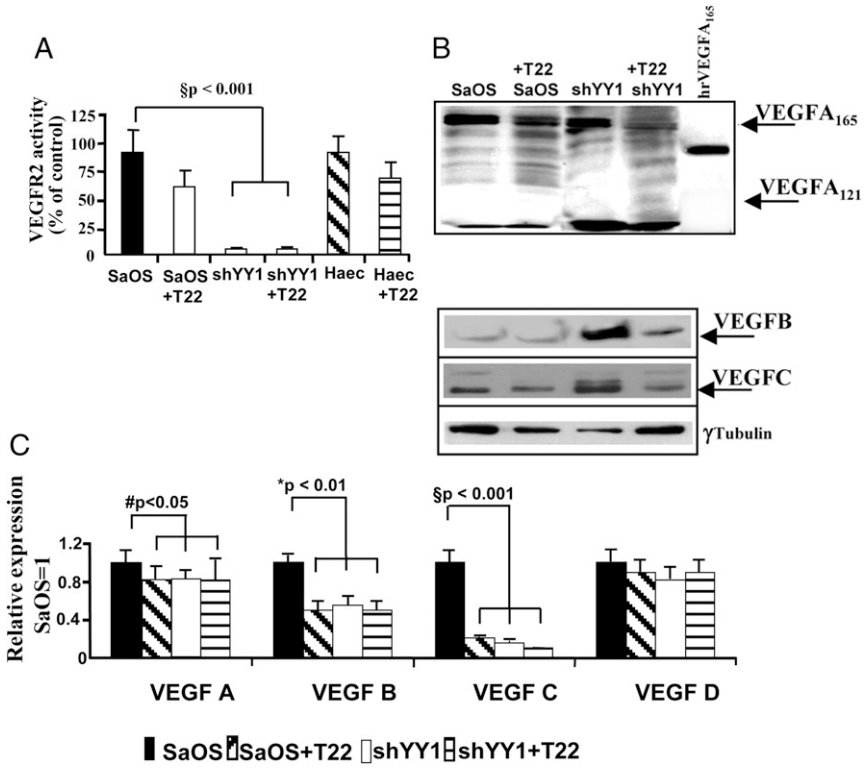

Fig. 3. Effect of T22 peptide and YY1 silencing on VEGF expression. (*A*) Media (100 μL/sample) from cultured cells were analyzed by a specific VEGFR2 inhibition assay. Data are presented as percentage of control activation. The mean ± SD of data from three independent experiments is shown. $^{\S}P < 0.001$ vs. SaOS. (*B*) Representative Western blots of total protein extracts from SaOS cells and shYY1 cells, untreated or treated with T22 peptide, revealed with VEGFA, -B and -C antibodies. (*C*) Real-time PCR quantification of VEGF transcripts performed on total RNA extracts from untreated SaOS cells, SaOS cells treated with T22 peptide, untreated shYY1 cells, and shYY1 cells treated with T22 peptide and normalized with GAPDH. SaOS transcripts were considered equal to 1, and the relative fold of the other transcripts was reported. Data shown are the mean ± SD from three independent experiments. $^{*}P < 0.01$, $^{\#}P < 0.05$, and $^{\S}P < 0.001$ vs. SaOS.

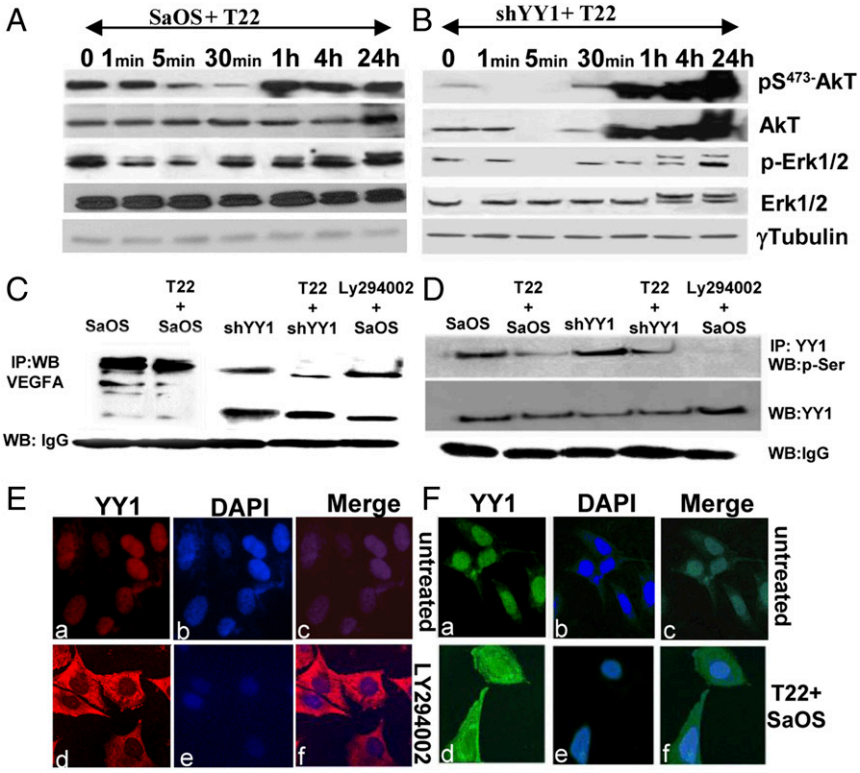

Fig. 5. T22 peptide blocks YY1 activity by impairing its serine phosphorylation via AKT. (*A* and *B*) Western blots of total protein extracts from SaOS and shYY1cells treated with T22 peptide at different time points revealed with specific antibodies, as indicated. Tubulin was used as loading control. (*C*) VEGFA protein expression in SaOS cells after treatment with T22 peptide and LY294002 inhibitor as indicated in figure. (*D*) Total protein extracts from SaOS cells untreated or treated with 100 nM T22 peptide and LY294002 inhibitor were immunoprecipitated with YY1 and immunoblotted with p-serine antibodies or immunoprecipitated with p-serine and immunoblotted with YY1. (*E*) Immunofluorescence of YY1 protein in SaOS cells and in SaOS cells treated with AKT inhibitor for 15 min (20× magnification, confocal microscope). DAPI was used for nuclear staining. (*a*) SaOS cells stained with YY1 antibodies. (*b*) SaOS nuclei stained with DAPI. (*c*) Merge. (*d*) SaOS cells treated with LY294002 for 15 min (*Materials and Methods*) stained with YY1 antibodies. (*e*) SaOS nuclei stained with DAPI. (*f*) Merge. (*F*) Immunofluorescence of YY1 protein in untreated SaOS cells and in SaOS cells treated with T22 peptide for 4 h (20× magnification). (*a*) SaOS cells stained with YY1 antibodies. (*b*) SaOS nuclei stained with DAPI. (*c*) Merge. (*d*) SaOS cells stained with YY1 antibodies after treatment with T22 peptide. (*e*) SaOS nuclei stained with DAPI. (*f*) Merge.

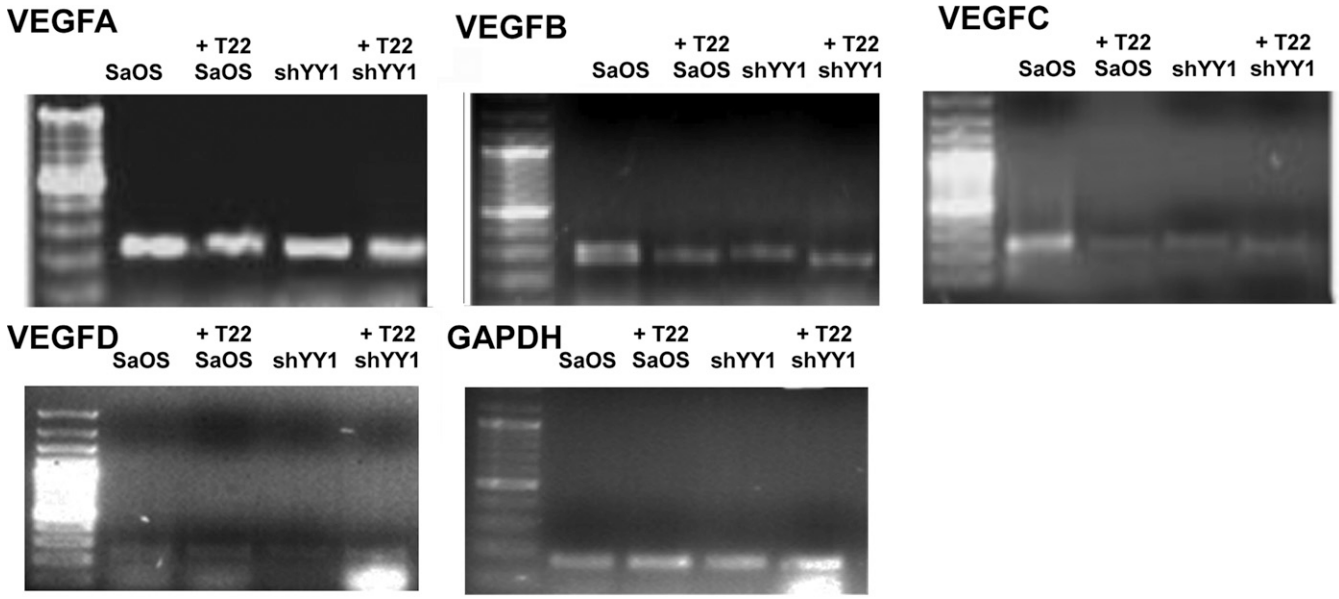

Fig. S3. Representative RT/PCRs with primer pairs for specific VEGF transcripts as indicated and performed on total RNA from SaOS cells, T22 peptide-treated SaOS cells, shYY1 cells, and shYY1 cells treated with T22 peptide.

Published online March 25, 2019.

www.pnas.org/cgi/doi/10.1073/pnas.1902206116

CORRECTION

CXCR4/YY1 inhibition impairs VEGF network and angiogenesis during malignancy

Filomena de Nigris[a], Valeria Crudele[a], Alfonso Giovane[b], Amelia Casamassimi[a], Antonio Giordano[c,d], Hermes J. Garban[e], Francesco Cacciatore[f], Francesca Pentimalli[c], Diana C. Marquez-Garban[e], Antonella Petrillo[g], Letizia Cito[c], Linda Sommese[a], Andrea Fiore[a], Mario Petrillo[g], Alfredo Siani[g], Antonio Barbieri[h], Claudio Arra[h], Franco Rengo[f], Toshio Hayashi[i], Mohammed Al-Omran[j], Louis J. Ignarro[j,k,1], and Claudio Napoli[a,j,1]

[a]Division of Clinical Pathology, Department of General Pathology, [b]Department of Biochemistry and Biophysics, School of Medicine, Second University of Naples, 80138 Naples, Italy; [f]Division of Geriatrics, Federico II University of Naples, 80131 Naples, Italy; [c]Sbarro Research Institute, College of Science and Technology, Temple University, Philadelphia, PA 19122; [d]Department of Human Pathology and Oncology, University of Siena, 53100 Siena, Italy; [e]Department of Medicine, Division of Dermatology and Division of Hematology–Oncology and Jonsson Comprehensive Cancer Center and [k]Department of Molecular and Medical Pharmacology, David Geffen School of Medicine, University of California, Los Angeles, CA 90095; [g]Unit of Radiology and [h]Animal Facility Unit, Fondazione G. Pascale, Istituto di Ricovero e Cura a Carattere Scientifico, 80131 Naples, Italy; [i]Department of Geriatrics, Nagoya University Graduate School of Medicine, 464-8601 Nagoya, Japan; and [j]Peripheral Vascular Disease Research Chair, College of Medicine, King Saud University, Riyadh 11472, Kingdom of Saudi Arabia

Contributed by Louis J. Ignarro, July 2, 2010 (sent for review January 20, 2010)

Tumor growth requires neoangiogenesis. VEGF is the most potent proangiogenic factor. Dysregulation of hypoxia-inducible factor (HIF) or cytokine stimuli such as those involving the chemokine receptor 4/stromal-derived cell factor 1 (CXCR4/SDF-1) axis are the major cause of ectopic overexpression of VEGF in tumors. Although the CXCR4/SDF-1 pathway is well characterized, the transcription factors executing the effector function of this signaling are poorly understood. The multifunctional Yin Yang 1 (YY1) protein is highly expressed in different types of cancers and may regulate some cancer-related genes. The network involving CXCR4/YY1 and neoangiogenesis could play a major role in cancer progression. In this study we have shown that YY1 forms an active complex with HIF-1α at VEGF gene promoters and increases VEGF transcription and expression observed by RT-PCR, ELISA, and Western blot using two different antibodies against VEGFB. Long-term treatment with T22 peptide (a CXCR4/SDF-1 inhibitor) and YY1 silencing can reduce in vivo systemic neoangiogenesis ($P < 0.01$ and $P < 0.05$ vs. control, respectively) during metastasis. Moreover, using an in vitro angiogenesis assay, we observed that YY1 silencing led to a 60% reduction in branches ($P < 0.01$) and tube length ($P < 0.02$) and a 75% reduction in tube area ($P < 0.001$) compared with control cells. A similar reduction was observed using T22 peptide. We demonstrated that T22 peptide determines YY1 cytoplasmic accumulation by reducing its phosphorylation via downregulation of AKT, identifying a crosstalk mechanism involving CXCR4/YY1. Thus, YY1 may represent a crucial molecular target for antiangiogenic therapy during cancer progression.

cancer | metastasis | oncogene

Angiogenesis is critical to the growth, invasion, and metastasis of human tumors (1, 2). Because targeting angiogenesis has emerged as a promising strategy for the therapeutic treatment of cancer, understanding the transcriptional regulation that determines the tumor angiogenic phenotype has become of cardinal importance (3).

Yin Yang 1 (YY1) protein has diverse roles in cancer development (4) including drug resistance (5, 6) and transcriptional regulation of many genes (7). YY1 also is involved in the regulation of angiogenesis during malignancy (8). Certainly, YY1 silencing reduced intrametastatic and systemic neoangiogenesis interacting with the chemokine receptor 4 (CXCR4) pathway in osteosarcoma (SaOS) cells (8). Interestingly, CXCR4 is required for cancer progression and blood supply via neoangiogenesis (9–11). Accordingly, some of CXCR4 inhibitors are being evaluated in clinical trials as adjunct therapy (12) (http://clinicaltrials.gov). The network that involves CXCR4/YY1 and neoangiogenesis could play a major role in cancer pathobiology. In this study, we demonstrate that YY1 has a crucial role during neoangiogenesis and elucidate the mechanism by which CXCR4/YY1 inhibition reduces VEGF-dependent neoangiogenesis.

Results

Effects of YY1 Silencing and CXCR4 Inhibition on Angiogenesis. To monitor angiogenesis in vivo and quantify the effects of YY1 silencing and/or CXCR4 inhibition (known to inhibit tumor growth), nude mice were inoculated with native or YY1-deleted (shYY1) human SaOS cells and treated with T22 peptide as control. Angiogenesis in vivo was monitored with Directed in Vivo Angiogenesis Assay (DIVAA) angioreactors implanted into the dorsal flank of mice following the schedule shown in Fig. S1. Tumor growth was monitored by NMR (Fig. 1*A*). The number and size of lung metastases were reduced by 70% in the mice injected with shYY11 cells as compared with the control group; moreover, they were negative to YY1 antibody, as revealed by immunohistochemistry (Fig. S2). To determine whether YY1 affected new vessel formation, angioreactors (Fig. 1*B*) and neoformed blood vessels were recovered from all mice at the end of treatment (Fig. 1*C*). Enhanced vessel growth was found within the lumen of angioreactors recovered from SaOS-injected mice (Fig. 1*B a* and *b*) as compared with angioreactors from mice treated with shYY1 cells or T22 peptide (Fig. 1*B c* and *d*). Cells in fresh vessels were quantified as FITC-lectin–positive by immunofluorescence. Fig. 1*D* indicates that T22 peptide and YY1 silencing reduce new blood vessel formation by about 50% ($P < 0.01$ vs. control and $P < 0.05$ vs. control, respectively), although T22 peptide was ineffective in further reducing vessel formation in mice injected with shYY1 cells. To examine the kinetic events underlying angiogenesis, we used an in vitro coculture model (13) in which SaOS or shYY1 cells were added to a monolayer of human aortic endothelial cells (HAEC)/fibroblasts (13). As shown in Fig. 2*A a–d*, SaOS cells organized a tubular structure after 48 h that was significantly reduced by the administration of T22 peptide (Fig. 2*A e*), whereas shYY1 cells showed only very small branches within the same time period (Fig. 2*A f–h*). We investigated the effects of YY1 silencing and T22 peptide treatment on angiogenesis by tube-formation

Author contributions: F.d.N., L.J.I., and C.N. designed research; F.d.N., V.C., A. Giovane, A.C., A. Giordano, F.C., A.P., L.C., L.S., A.F., M.P., A.B., C.A., T.H., and M.A.-O. performed research; A. Giordano, F.P., and L.C. contributed new reagents/analytic tools; F.d.N., V.C., A. Giovane, A.C., A. Giordano, H.J.G., F.C., F.P., D.C.M.-G., A.P., L.C., L.S., A.F., M.P., A.S., A.B., C.A., F.R., T.H., M.A.-O., L.J.I., and C.N. analyzed data; and F.d.N., H.J.G., F.C., L.J.I., and C.N. wrote the paper.

The authors declare no conflict of interest.

[1]To whom correspondence may be addressed. E-mail: lignarro@mednet.ucla.edu. or claunap@tin.it.

This article contains supporting information online at www.pnas.org/lookup/suppl/doi:10.1073/pnas.1008256107/-/DCSupplemental.

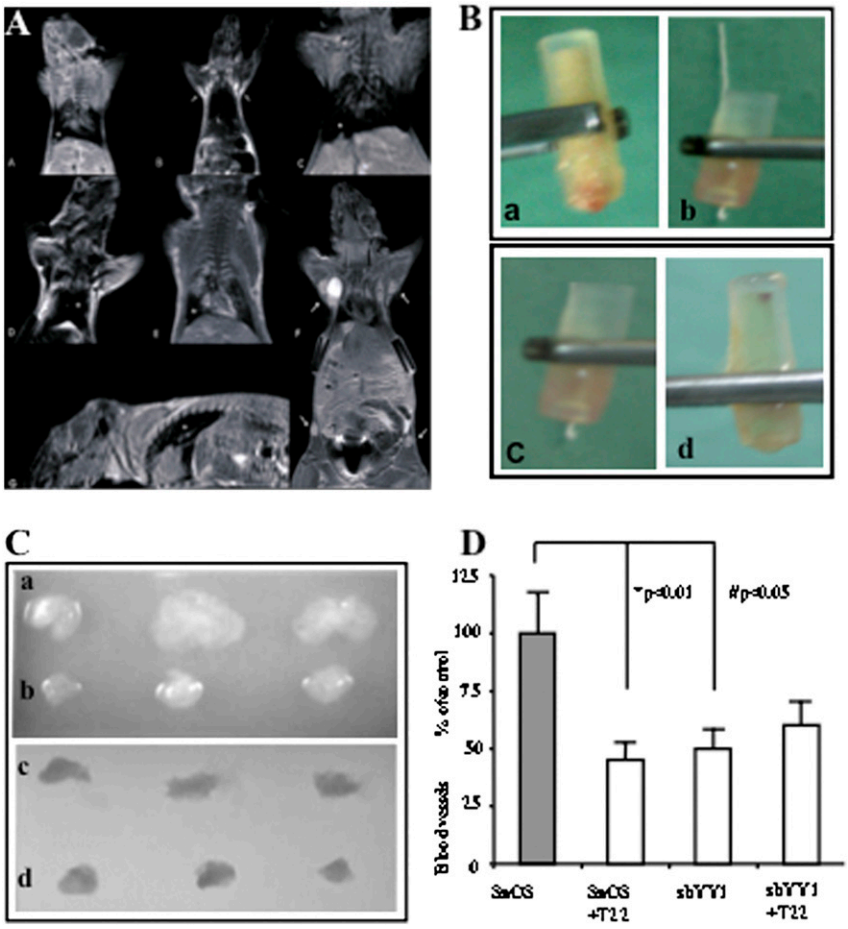

Fig. 1. The systemic angiogenic pathway responds to different treatments by producing vascular tissue within angioreactors lumen. (*A*) MRI assessment of lung and lymph node metastases. Coronal (*a–f*,) and sagittal (*g*) postcontrast T1-weighted images are shown. Lung metastases (*) and lymph node metastases (arrows) are well demonstrated on the T1-weighted images. (*B*) Representative images of angioreactors recovered 13 wk after implantation in SaOS mouse group (control) (*a*), SaOS mouse group after treatment with 100 nM of T22 peptide (*b*), shYY1 mouse group (*c*), and shYY1/T22– peptide treated mouse group (*d*). Mouse groups in *a* and *c* were treated with scrambled peptide. (*C*) Vessels were recovered from angioreactors and photographed: vessel mass from control SaOS-bearing mice (*a*), T22 peptide-treated SaOS-bearing mice (*b*), shYY1-bearing mice (*c*), and T22 peptide-treated shYY1-bearing mice (*d*). (*D*) Lectin fluorescence quantification of vessels 13 wk after implantation. Immunofluorescence intensity was measured and expressed relative to control mice inoculated with SaOS cells. Data are mean + SD; $n = 5$ independent mice per group with two angioreactors each. $^{*}P < 0.01$ and $^{\#}P < 0.05$ vs. SaOS.

assay (Fig. 2*B a–f*). All tube-like structures were positive for CD34 antibodies (Fig. 2*B h–l*). We also determined the number of branches per field and tube length and area (Fig. 2*C a–c*). YY1 silencing led to a 60% reduction in branch number and tube length, and tube area was reduced by 75% compared with SaOS cells. A similar reduction was observed using T22 peptide in SaOS cells, but no additive effect of T22 peptide was observed in shYY1 cells (Fig. 2*C a–c*).

YY1 Modulates VEGF Expression and Transcription in Vitro. We first measured the overall VEGF levels in cell media by ELISA (Table S1) and found that shYY1 cells secreted about 30% more VEGF than did SaOS cells (270 vs. 200 pg/mL); moreover, these levels were reduced by 50% 24 h after treatment with T22 peptide (10 ng/mL VEGF in coculture with SaOS cells and 11 ng/mL in coculture with shYY1 cells). However, VEGF secreted from shYY1 cells was less able to activate its receptor VEGFR2 (reduced by 70%) than VEGF secreted from SaOS or endothelial cells (Fig. 3*A*), suggesting that YY1 silencing increases the release of VEGF isoforms that are inactive on VEGFR2 (14). Western blot analysis performed on total cell extracts (Fig. 3*B*) showed the presence of VEGFA in SaOS cells by two main bands compatible with VEGFA165 and VEGFA121 molecular weight. YY1 silencing increased the VEGFA121 isoform and down-regulated VEGFA165, which also was reduced by treatment withT22 peptide. VEGFB was more abundant in shYY1 cells at high molecular weight, indicating that this subform probably contains posttraslational modifications or an alternative splicing. VEGFC was detected as two bands around 25 kDa; their relative expression increased after treatment with T22 peptide and YY1 silencing (Fig. 3*B*). We believe that the upper band may be a posttranslational modification of the lower one. It is noteworthy that these observations were obtained with two different antibodies. These data indicate that YY1 silencing alters the expression pattern of VEGF isoforms in osteosarcoma, resulting in an inactive cascade on VEGFR2.

Real-time PCR, performed on common exons of all isoforms from different VEGF genes, revealed that their mRNAs were enriched selectively in SaOS cells and down-regulated in shYY1-cells. As shown in Fig. 3*C* and Fig. S3, VEGFA transcript was reduced by 20% after treatment with T22 peptide and YY1 silencing. VEGFB was reduced by 50% with treatment with T22 peptide and/or YY1 silencing. The strongest effect was observed on the VEGFC transcription level, which was ≈80% lower in shYY1- and T22-treated cells (Fig. 3*C* and Fig. S3). No additive effect was observed with T22 peptide and YY1 silencing double treatment. We hypothesized that YY1 can regulate VEGF genes directly but also interferes with the signal transduction pathway involved in post-translational modifications of VEGF proteins. To test this hypothesis, we first characterized the regulatory elements of VEGF genes. We inserted 2 kb of the genomic 5′ UTR of the *VEGFA*, *-B*, and *-C* genes into the pGL3 vector and an in vitro luciferase-reporter gene assay for analysis. We found that YY1 silencing and/or treatment with T22 peptide reduced luciferase activity in all isoforms, with highly significant reductions for the VEGFB and -C regulatory regions (Fig. 4*A*). The sequence analysis of the 2-kb 5′ regulatory regions of the *VEGFA*, *-B*, and *-C* genes revealed potential YY1 binding sites at positions -1660 of *VEGFA*, -420 of *VEGFB*, and -390 and -380 of *VEGFC* (Fig. 4*B*). No hypothetical YY1 binding sites were detected for *VEGFD* using the same score.

Chromatin preparations isolated from SaOS cells were immunoprecipitated using anti-YY1 and anti-basal transcription factor II D (TFIID) antibodies, and immunoprecipitated genomic frag-

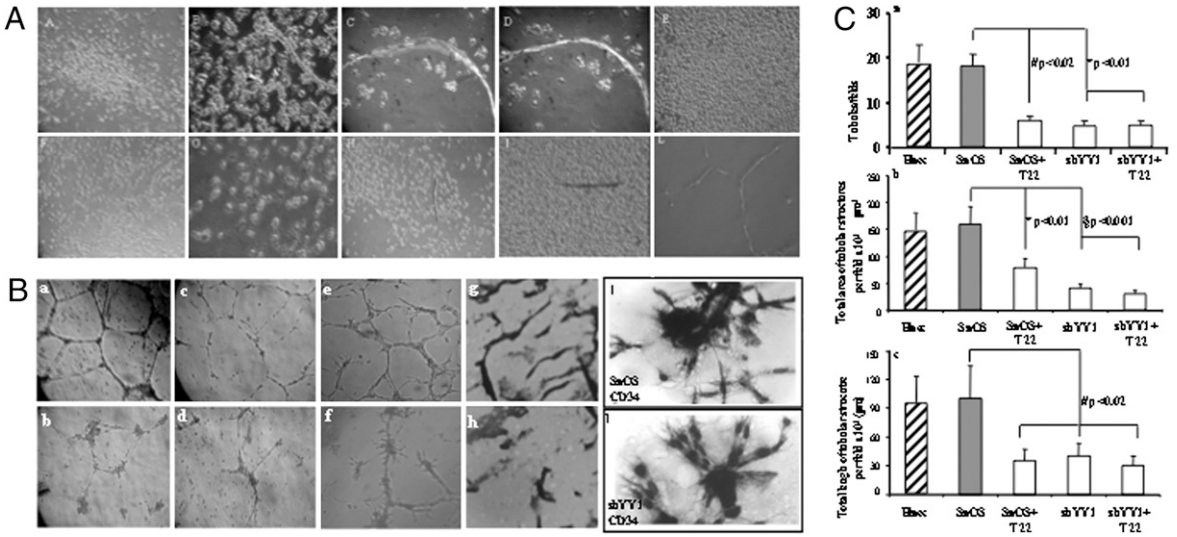

Fig. 2. In vitro angiogenesis assay: the effect of treatment with T22 peptide and shYY1 silencing. (*A*) HAEC/fibroblast monolayer was cultured on Matrigel for 24 h; then SaOS or shYY1 cells were added to the culture with Opti-MEM medium without VEGF and basic fibroblast growth factor for 24 h (details are given in *SI Materials and Methods*). Cells were photographed, at different time points. (*a*) SaOS cells after 2 h of coculture. (*b*) SaOS coculture after 8 h. (*c*) SaOS coculture after 24 h. (*d*) SaOS coculture after 48 h. (*e*) SaOS coculture treated with T22 peptide after 24 h. (*f*) shYY1 cells plated on HAEC/fibroblast monolayer after 2 h. (*g*) shYY1 coculture after 24 h. (*h*) shYY1 cells cocultured after 48 h. (*i*) shYY1 coculture treated with T22 peptide after 24 h. (*l*) HAEC cells after 48 h. (*B*) HAEC cells (1×10^4/well) were plated on 24-well Matrigel-coated plates. After 2 h, 1×10^4 SaOS or shYY1 cells were stratified and cultured in minimum medium for 24 h, with or without 100 nM T22 peptide. Then cells were photographed, and tube formation was quantified with ImageJ analysis software. (*a*) SaOS cells. (*b*) SaOS cells treated with T22 peptide. (*c*) shYY1 cells. (*d*) shYY1 cells treated with T22 peptide. (*e*) HAEC cells in minimum medium without VEGF after 24 h. (*f*) HAEC cells treated with T22 peptide. (*g*) CD34 staining of SaOS coculture. (*h*) CD34 staining of shYY1 coculture. (*i*) SaOS cells and (*l*) shYY1 cocultures stained with CD34 (20× magnification). (*C*) HAEC cells were plated on Matrigel. Then SaOS or shYY1 cells were added with Opti-MEM medium without VEGF for 24 h. Four fields at 20× magnification were photographed, and tube formation was quantified with image analysis software, as described in *Material and Methods*. Tube junctions (*a*), area (*b*), and length (*c*), were quantified in at least four fields per sample and graphed as the mean ± SD, $^{*}P < 0.01$, $^{\#}P < 0.02$, and $^{\S}P < 0.001$ vs. SaOS.

ments then were amplified using specific primers spanning VEGFA, VEGFB, and VEGFC regulatory elements, as indicated in Fig. 4*B a*. ChIP assays revealed that YY1 binds all 5′ flanking regions of VEGFA, -B, and -C at the predicted sites (Fig. 4*B b*). To understand how much YY1 was present on each regulatory element of VEGFA, -B, and -C and whether YY1 silencing or treatment with T22 peptide influenced YY1 binding in vivo, we then performed a quantitative occupancy experiment. Chromatin from untreated and treated SaOS cells was immunoprecipitated using anti-YY1 antibody and amplified by real-time PCR using specific primers as shown (Fig. 4*B a*). Our results revealed that YY1 was present at a relatively low level on the VEGFA regulatory region; moreover, treatment with T22 peptide, YY1 silencing, or the combined treatment reduced chromatin occupancy by only 10% (Fig. 4*C a*). YY1 was enriched selectively on the putative regulatory element of VEGFB and -C in SaOS cells. Treatment with T22 peptide, YY1 silencing, or the combined treatment significantly reduced YY1 abundance on VEGFC and -B regulatory sequences (by 80% and 50%, respectively) compared with SaOS cells (Fig. 4*C a–c*). Consistently, treatment with T22 peptide, YY1 silencing, or combined treatment produced the same effect on YY1 promoter occupancy.

To examine whether there was simultaneous occupancy of VEGF regulatory regions by hypoxia-inducible factor 1α (HIF-1α) and YY1, as part of a transcriptional complex, we analyzed HIF-1α/YY1 coimmunoprecipitates from SaOS cell extracts. We found that HIF-1α was constitutively activated in SaOS cells; however, neither YY1 silencing nor treatment with T22 peptide influenced its expression (Fig. 4*D*). HIF-1 α and YY1 were present in the same immunocomplexes (Fig. 4*D*). These results suggest that YY1 positively cooperates with HIF-1α to regulate VEGFs expression.

CXCR4 and YY1 Transduction Pathway. We have observed a significant functional similarity between the SaOS cells treated with either shYY1 or T22 peptide. Thus, we have hypothesized that T22 peptide and YY1 could have a common pathway regulating VEGF proteins. Western blot showed that AKT was phosphorylated at S473 in SaOS cells (Fig. 5*A* and *B*) but was dramatically decreased in shYY1 cells and at early time points following treatment with T22 peptide. The inhibition of AKT also correlated with VEGFA reduction, as shown in LY294002-treated SaOS and in shYY1 cells (Fig. 5*C*), indicating that YY1 also promotes the accumulation of VEGF protein through AKT signaling (15). To investigate the direct cross talk between AKT and YY1, we analyzed the phosphorylation status of YY1 after treatment with T22 peptide and the PI3K kinase inhibitor Ly29004. By immunoprecipitation analysis we found that both treatments reduced the amount of the serine-phosphorylated form of YY1 in SaOS cells (Fig. 5*D*). Immunofluorescence analysis revealed an accumulation of YY1 in the cytoplasm of T22 peptide- and Ly29004-treated cells (Fig. 5 *E–F*). In addition, YY1 and AKT were present in the same immunocomplex (Fig. S4). Overall, these results suggest direct cross talk between YY1 and AKT, which may be involved in YY1 phosphorylation.

Discussion

In this study, we showed that (*i*) YY1 promotes neoangiogenesis, acting as a positive regulator of VEGF transcription; (ii) CXCR4 inhibition or YY1 silencing can reduce vessel density via VEGF through AKT down-regulation; (*iii*) reduced levels of AKT impair YY1 serine phosphorylation and its accumulation in cytoplasm.

It generally is accepted that angiogenesis is a rate-limiting process in tumor growth (16). Over the last few years, several clinical trials have demonstrated the clinical benefits conferred by anti-angiogenic agents for cancer treatment (17). However, recent

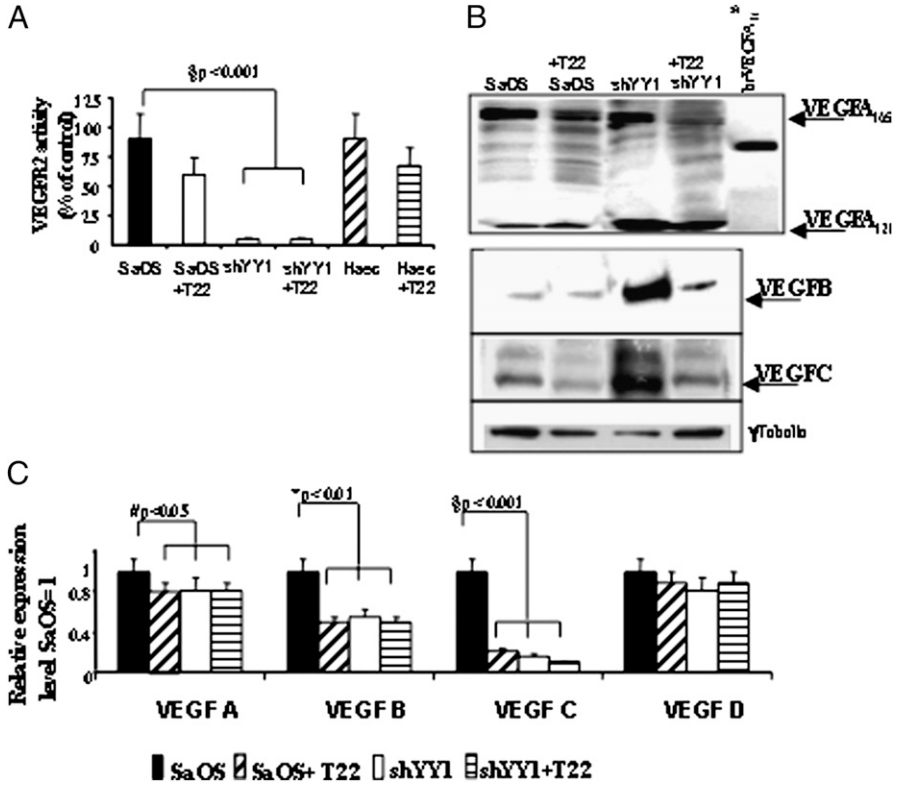

Fig. 3. Effect of T22 peptide and YY1 silencing on VEGF expression. (*A*) Media (100 μL/sample) from cultured cells were analyzed by a specific VEGFR2 inhibition assay. Data are presented as percentage of control activation. The mean ± SD of data from three independent experiments is shown. $^{\S}P < 0.001$ vs. SaOS. (*B*) Representative Western blots of total protein extracts from SaOS cells and shYY1 cells, untreated or treated with T22 peptide, revealed with VEGFA, -B and -C antibodies. (*C*) Real-time PCR quantification of VEGF transcripts performed on total RNA extracts from untreated SaOS cells, SaOS cells treated with T22 peptide, untreated shYY1 cells, and shYY1 cells treated with T22 peptide and normalized with GAPDH. SaOS transcripts were considered equal to 1, and the relative fold of the other transcripts was reported. Data shown are the mean ± SD from three independent experiments. $^{*}P < 0.01$, $^{\#}P < 0.05$, and $^{\S}P < 0.001$ vs. SaOS.

clinical data advance the possibility that VEGF blockade may result in an invasive phenotype of the tumor and may lead to the development of resistance (18). Various molecular members of the VEGF and chemokine signaling pathway have been implicated in the incomplete response to VEGFA blockers (19), suggesting the need to investigate the mechanisms of VEGF regulation. In this study we have investigated the role of YY1 (20) and the CXCR4 pathway during neoangiogenesis in vivo and their involvement in the mechanism of VEGF regulation. VEGF exists in multiple isoforms, and different expression patterns are documented in different tumors (21). We previously demonstrated that CXCR4 and/or YY1 inhibition reduced in vivo angiogenesis by inhibiting neovessel formation in vivo as well as cell migration and invasion in vitro (8). Here, consistent with previous results, we show that CXCR4 inhibition or YY1 silencing can reduce vessel density and tubular structures in vitro through the decreased expression of conventional proangiogenic VEGFA165 protein. Moreover, we found that YY1 silencing (acting both at transcriptional and posttranslational levels) alters the expression pattern of VEGF in osteosarcoma by producing VEGFB and -C isoforms that cannot activate the receptor VEGFR2 in vitro (14). We demonstrated that YY1, together with HIF-1α, binds its target sequences on the regulatory regions of VEGFA, -B, and -C, acting as an activator in all of them. However, YY1 silencing also resulted in down-regulation of AKT kinase (22); this finding could account for the reduction of VEGFA protein and for the accumulation of aberrant isoforms of VEGFB and -C. Indeed, levels of VEGFB and -C protein did not correlate with the observed mRNAs. Recently, it has been shown that YY1 regulates important targets of cancer therapy, such as drug resistance gene (6) or death receptor (5). Our findings identify VEGF as a target of YY1. Moreover, we identified YY1 as a downstream effector molecule of the CXCR4/SDF-1 pathway controlled by AKT. Down-regulation of AKT by T22 peptide or AKT inhibition decreased YY1 phosphorylation necessary for its nuclear localization and transcriptional activity (23, 24). In addition to several well-documented mechanisms of YY1 transcription activity (4), we here demonstrate the relevance of YY1 serine phosphorylation in the cellular signaling modulated by AKT.

Currently, there is no specific compound targeting YY1 (6, 25). In contrast, eight preclinical metastatic models demonstrated the efficacy of CXCR4 inhibitors that are moving to clinical trials (8). Our data indicate that T22, a CXCR4-blocking peptide, also acts by deactivating the multifunctional transcription factor YY1. We know that the therapeutic benefit associated with anti-VEGF–targeted therapy is complex and involves multiple mechanisms (26). A better understanding of these mechanisms will lead to future advances in the use of these agents in clinical practice. Our results establish that YY1 promotes neoangiogenesis, acting as a positive coregulator of VEGF transcription and/or affecting its translation via AKT. YY1 can be considered a marker for stratifying patients better and as an additional therapeutic strategy to reduce neoangiogenesis and tumor growth.

Materials and Methods

Cell Lines, Treatments, and Transfections. SaOS and shYY1-SaOS cell lines were cultured and maintained as described (10). HAEC cells (ATCC) were grown in EGM-2 medium (GIBCO). T22 peptide was used at a concentration of 100 nM for 24 h in the in vitro assays. A 2-kb segment of the 5′ UTR of VEGF genes

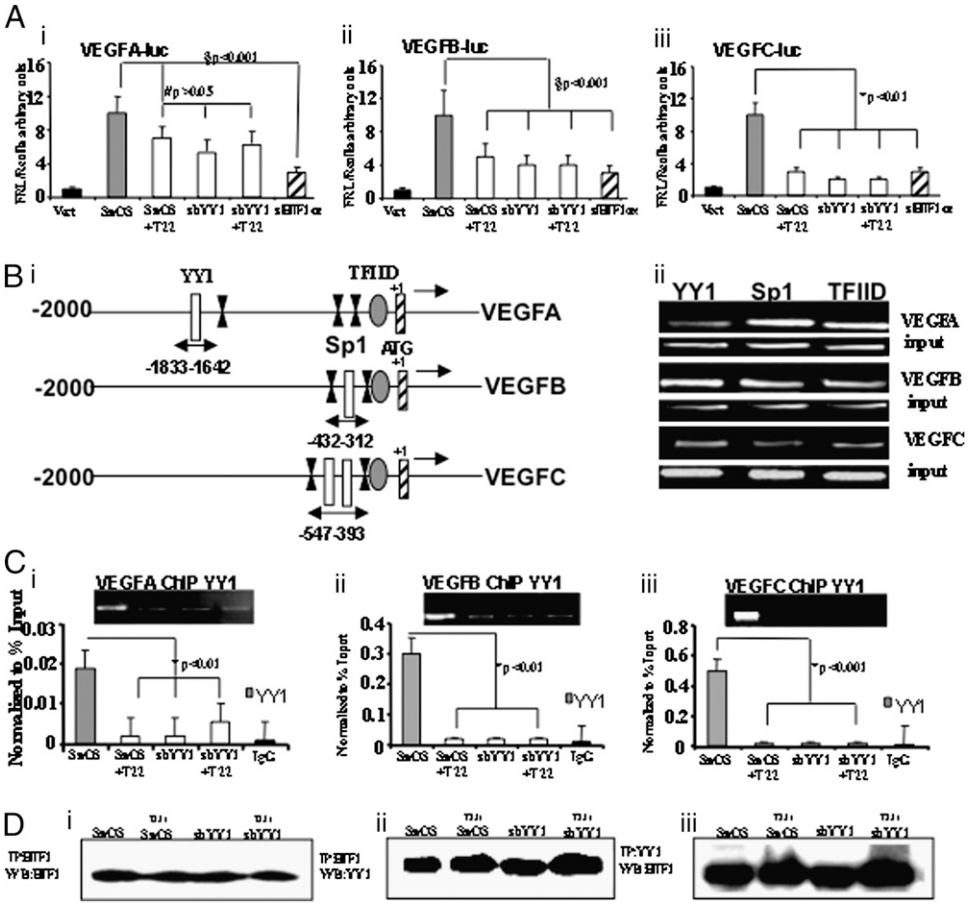

Fig. 4. YY1 is a positive regulator of VEGF transcription. (*A*) VEGF promoter activity. SaOS and shYY1 cells, untreated or treated with T22 peptide, were transiently cotransfected with VEGF luciferase constructs and PRL-SV40. The amount of transfected DNA was maintained at 1.5 μg/well by the addition of the appropriated amount of the empty vector. After 48 h, cells were harvested for dual-luciferase assays. The relative promoter activity (fold) was the ratio of luciferase (Firefly/Renilla) value relative to SaOS cell value. Data represent the mean of three experiments ± SD. (*a*) VEGFA promoter activity. Treatment with T22 peptide and YY1 silencing reduced luciferase activity by only 15%, and differences were not significant compared with SaOS ($^{\#}P > 0.05$). HIF reduced VEGFA promoter activity by 80% compared with SaOS (§HIFα vs. SaOS, $P < 0.001$). (*b*) Luciferase assays of VEGFB regulatory element. VEGFB promoter activity was reduced by 50% in SaOS cells and in shYY1 cells after treatment with T22 peptide ($^{\S}P < 0.001$ vs. SaOS); treatment with T22 peptide and YY1 silencing had no additive effect. HIF reduced luciferase activity by 80% ($^{\S}P < 0.001$ vs. SaOS). (*c*) Luciferase assays of VEGFC regulatory element. T22 peptide in SaOS cells reduced luciferase activity and YY1 silencing by 70% ($^{*}P < 0.01$ vs. SaOS). Treatment with T22 peptide and YY1 silencing had no additive effect. HIF reduced luciferase activity by 80% ($^{*}P < 0.01$ vs. SaOS). (*B*) (*a*) VEGFA, -B, and -C 5′ flanking regions of the VEGF transcription start site and hypothetical binding sites for YY1, Sp1, and TFIID. Nucleotide positions relative to the transcription start site are shown above the gene. (*b*) ChIP assays performed on VEGFA, -B, and -C regulatory elements. Chromatin from SaOS cells was immunoprecipitated with YY1, Sp1, and TFIID antibodies and amplified with primers spanning VEGF regulatory element binding sites. (*C*) Occupancy of YY1 at the VEGFA, -B, and -C binding sites was analyzed by ChIP in SaOS and shYY1 cells untreated or treated with T22 peptide. ChIP was performed using an antibody against YY1α or a nonspecific control. Immunoprecipitated DNA was quantified by real-time PCR using the indicated primer sets; GAPDH primers were used as control. Data are reported as the fold enrichment in the YY1 immunoprecipitation relative to the control. The means ± SD of data from three independent experiments are shown ($^{*}P$ <0.01 vs. SaOS). (*D*) Western blots of protein extracts from the indicated cells revealed with HIF1α (*a*). Protein extracts immunoprecipitated with HIF1α antibodies and revealed with YY1 (*b*). YY1 immunoprecipitates revealed with HIF1α antibodies (c).

(NM_003376, NM_003377, NM_005429) was amplified, inserted into the pGL3 vector, and assayed by dual-luciferase assays (*SI Materials and Methods*).

Tube Formation Assay. HAEC cells (1×10^4 cells/well) were seeded in 24-well Matrigel-coated culture plates; after 24 h, 1×10^3 human fibroblasts were stratified; finally 1×10^4 shYY1 cells were added in the presence or absence of 100 nM T22 peptide and were cultured in Opti-MEM (Invitrogen). The number of tubes, total length, and area per low-powered field (20×) for each well were analyzed using NIS Elements software (Nikon, Inc). Tubular structures were stained with a CD34 monoclonal antibody as described (8).

VEGF Dosage by ELISA. Dosage of VEGF in culture media was performed using Human VEGF ELISA kit (Orgenium Laboratories) following the manufacturer's recommendations.

Western Blotting and Immunoprecipitation. Whole-cell extracts were tested with specific antibodies (*SI Materials and Methods*).

In Vivo Experiments and Direct Angiogenesis in Vivo Assay. In vivo experiments were carried out in accordance with the institutional animal care guidelines and were compliant with national (Ministero della Salute, Rome, Italy) and international (European Community and National Institutes of Heath, Bethesda, MD) laws. Vessels were treated using the Trevigen DIVAA kit as described (8) (*SI Materials and Methods*).

ChIP Assays and Real-Time PCR. ChIP assays were performed as described (10). Immunoprecipitated DNA was analyzed by real-time PCR using SYBR Green detection. Primer details are given in *SI Materials and Methods* and Table S2.

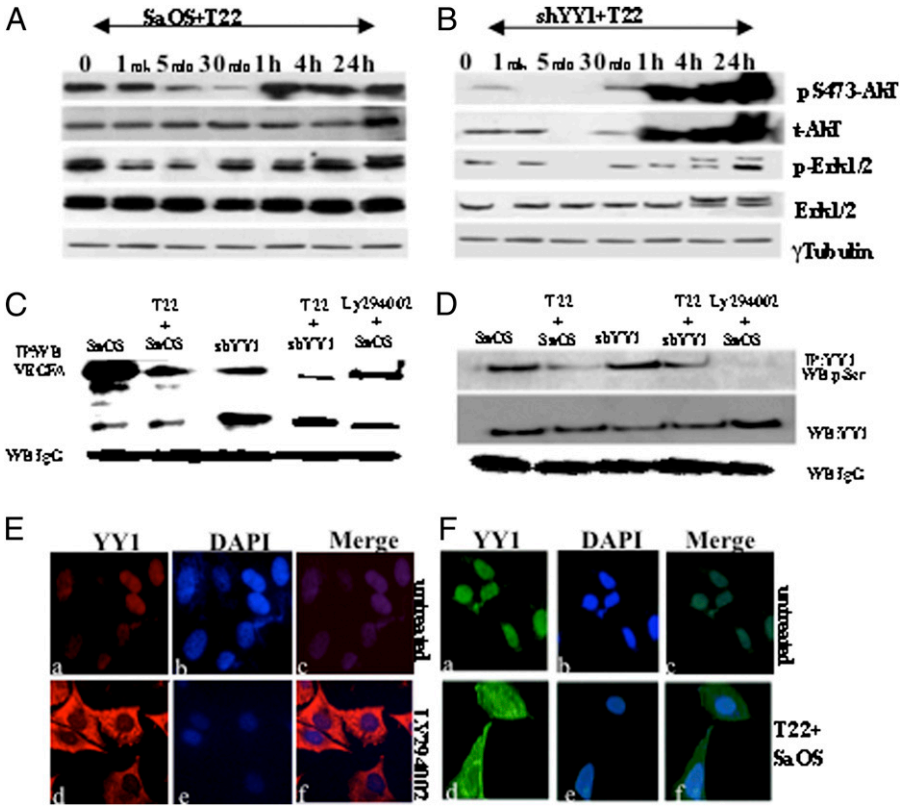

Fig. 5. T22 peptide blocks YY1 activity by impairing its serine phosphorylation via AKT. (*A* and *B*) Western blots of total protein extracts from SaOS and shYY1cells treated with T22 peptide at different time points revealed with specific antibodies, as indicated. Tubulin was used as loading control. (*C*) VEGFA protein expression in SaOS cells after treatment with T22 peptide and LY294002 inhibitor as indicated in figure. (*D*) Total protein extracts from SaOS cells untreated or treated with 100 nM T22 peptide and LY294002 inhibitor were immunoprecipitated with YY1 and immunoblotted with p-serine antibodies or immunoprecipitated with p-serine and immunoblotted with YY1. (*E*) Immunofluorescence of YY1 protein in SaOS cells and in SaOS cells treated with AKT inhibitor for 15 min (20× magnification, confocal microscope). DAPI was used for nuclear staining. (*a*) SaOS cells stained with YY1 antibodies. (*b*) SaOS nuclei stained with DAPI. (*c*) Merge. (*d*) SaOS cells treated with LY294002 for 15 min (*Materials and Methods*) stained with YY1 antibodies. (*e*) SaOS nuclei stained with DAPI. (*f*) Merge. (*F*) Immunofluorescence of YY1 protein in untreated SaOS cells and in SaOS cells treated with T22 peptide for 4 h (20× magnification). (*a*) SaOS cells stained with YY1 antibodies. (*b*) SaOS nuclei stained with DAPI. (*c*) Merge. (*d*) SaOS cells stained with YY1 antibodies after treatment with T22 peptide. (*e*) SaOS nuclei stained with DAPI. (*f*) Merge.

Statistical Analysis. Data were analyzed by using the SPSS 13.0 statistical package. Data are presented as mean ± SD. Differences were evaluated by Student's *t* test. $P < 0.05$ was considered statistically significant.

ACKNOWLEDGMENTS. This work was supported by Grants 0622153_002 and 2008T85HLH_002 from the Progetto di Rilevante Interesse Nazionale Ministero Italiano Università e Ricerca 2006 and 2008 to the II University of Naples (C.N.).

1. Hanahan D, Folkman J (1996) Patterns and emerging mechanisms of the angiogenic switch during tumorigenesis. *Cell* 86:353–364.
2. Bergers G, Benjamin LE (2003) Tumorigenesis and the angiogenic switch. *Nat Rev Cancer* 3:401–410.
3. Grothey A, Galanis E (2009) Targeting angiogenesis: Progress with anti-VEGF treatment with large molecules. *Nat Rev Clin Oncol* 6:507–518.
4. Gordon S, Akopyan G, Garban H, Bonavida B (2006) Transcription factor YY1: Structure, function, and therapeutic implications in cancer biology. *Oncogene* 25:1125–1142.
5. Garbán HJ, Bonavida BJ (2001) Nitric oxide inhibits the transcription repressor Yin-Yang 1 binding activity at the silencer region of the Fas promoter: A pivotal role for nitric oxide in the up-regulation of Fas gene expression in human tumor cells. *J Immunol* 167:75–81.
6. Baritaki S, et al. (2008) Inhibition of Yin Yang 1-dependent repressor activity of DR5 transcription and expression by the novel proteasome inhibitor NPI-0052 contributes to its TRAIL-enhanced apoptosis in cancer cells. *J Immunol* 180:6199–6210.
7. Sui G, et al. (2004) Yin Yang 1 is a negative regulator of p53. *Cell* 117:859–872.
8. de Nigris F, et al. (2008) Deletion of Yin Yang 1 protein in osteosarcoma cells on cell invasion and CXCR4/angiogenesis and metastasis. *Cancer Res* 68:1797–1808.
9. Wong D, Korz W (2008) Translating an antagonist of chemokine receptor CXCR4: From bench to bedside. *Clin Cancer Res* 14:7975–7980.
10. de Nigris F, et al. (2007) Cooperation between Myc and YY1 provides novel silencing transcriptional targets of alpha3beta1-integrin in tumour cells. *Oncogene* 26:382–394.
11. Zlotnik A (2008) New insights on the role of CXCR4 in cancer metastasis. *J Pathol* 215:211–213.
12. Hotte SJ, et al. (2008) A phase 1 study of mapatumumab (fully human monoclonal antibody to TRAIL-R1) in patients with advanced solid malignancies. *Clin Cancer Res* 14:3450–3455.
13. Staton CA, Reed MW, Brown NJ (2009) A critical analysis of current in vitro and in vivo angiogenesis assays. *Int J Exp Pathol* 90:195–221.
14. Ferrara N, Gerber HP, LeCouter J (2003) The biology of VEGF and its receptors. *Nat Med* 9:669–676.
15. Liang Z, et al. (2007) CXCR4/CXCL12 axis promotes VEGF-mediated tumor angiogenesis through Akt signaling pathway. *Biochem Biophys Res Commun* 359:716–722.
16. Kerbel RS (2008) Tumor angiogenesis. *N Engl J Med* 358:2039–2049.
17. Ellis LM, Hicklin DJ (2008) VEGF-targeted therapy: Mechanisms of anti-tumour activity. *Nat Rev Cancer* 8:579–591.
18. Chen HX, Cleck JN (2009) Antiangiogenic clinical strategies: Adverse effect of anticancer agents that target the VEGF pathway. *Nat Rev Clin Oncol* 6:465–477.
19. Crawford Y, Ferrara N (2009) Tumor and stromal pathways mediating refractoriness/resistance to anti-angiogenic therapies. *Trends Pharmacol Sci* 30:624–630.
20. de Nigris F, et al. (2006) Expression of transcription factor Yin Yang 1 in human osteosarcomas. *Eur J Cancer* 42:2420–2424.
21. Harper SJ, Bates DO (2008) VEGF-A splicing: The key to anti-angiogenic therapeutics? *Nat Rev Cancer* 8:880–887.
22. Petrella BL, Brinckerhoff CE (2009) PTEN suppression of YY1 induces HIF-2 activity in von-Hippel-Lindau-null renal-cell carcinoma. *Cancer Biol Ther* 8:1389–1401.
23. Austen M, Luscher B, Luscher-Firzlaff JM (1997) Charaterization of transcription regulator YY1. *J Biol Chem* 272:1709–1717.
24. Rizkallah R, Hurt MM (2009) Regulation of the transcription factor YY1 in mitosis through phosphorylation of its DNA-binding domain. *Mol Biol Cell* 20:4766–4776.
25. Huerta-Yepez S, et al. (2009) Nitric oxide sensitizes tumor cells to TRAIL-induced apoptosis via inhibition of the DR5 transcription repressor Yin Yang 1. *Nitric Oxide* 20:39–52.
26. Balestrieri ML, Napoli C (2007) Novel challenges in exploring peptide ligands and corresponding tissue-specific endothelial receptors. *Eur J Cancer* 43:1242–1250.